Springer

Journal of
Mechanical
Science and
Technology

Journal of Mechanical Science and Technology 22 (2008) 514~521

www.springerlink.com/content/1738-494x

Mass production of 3-D microstructures using projection microstereolithography

Young Myoung Ha[1], Jae Won Choi[2] and Seok Hee Lee[3,*]

[1]*Research Institute of Mechanical Technology, Pusan National University, San 30 Jangjeon-dong, Geumjeong-gu, Busan 609-735, Korea*

[2]*W.M. Keck Center for 3D Innovation, The University of Texas at El Paso, El Paso, TX 79902, USA*

[3]*School of Mechanical Engineering, Pusan National University, San 30 Jangjeon-dong, Geumjeong-gu, Busan 609-735, Korea*

(Manuscript Received May 16, 2007; Revised August 21, 2007; Accepted August 21, 2007)

Abstract

Microstereolithography (MSL) technology is derived from the conventional stereolithography process and can meet the demands for fabricating complex 3-D microstructures with high resolution. This technology can be divided into scanning and projection methods, which have different levels of precision and fabrication speeds. Scanning MSL fabricates very fine 3-D microstructures by controlling the position of the laser spot on the resin surface. Projection MSL quickly fabricates one layer with one exposure using a mask. In this paper, we propose a projection MSL system with uniform illumination and image formation based on optical design for fabricating microstructure arrays. This system can realize mass production of 3-D microstructures in the meso-range, which falls between micro- and macro-ranges, with a resolution of a few microns. Microstructure arrays were fabricated to verify the performance of the proposed system.

Keywords: Microstereolithography; Microstructure arrays; Mass production

1. Introduction

The demands for ultraprecision components, such as information and communication devices, micromechanical parts and medical devices, have increased. However, existing technologies, such as MEMS and LIGA, have had difficulties coping with the number of masks and fabricable heights. Microstereolithography (MSL) can meet these demands because it does not require masks and can be used to fabricate 3-D microstructures with high aspect ratios. MSL is derived from the conventional stereolithography process and uses the same input format, STL. This technology can be divided into scanning and projection methods [1].

In the scanning method shown in Fig. 1(a), a microstructure is built by stacking each photopolymerized layer, controlling a well focused laser beam on the resin surface according to the sliced section shape. Ikuta and Kirowatari [2] reported the first scanning MSL system, which was known as the Integrated Harden Polymer Process. Since then, many researchers have improved the fabricable resolution and demonstrated a variety of 3-D microstructures using similar scanning MSL techniques [3-5].

In the projection method shown in Fig. 1(b), a microstructure is built by stacking each photopolymerized layer by using one irradiation of well patterned UV light on the resin surface according to the sliced section shape. Bertsch *et al*. [6] described a projection MSL system using a liquid crystal display (LCD) as the dynamic pattern generator. Projection MSL systems using LCDs have advanced so that they can now be used to fabricate diverse microstructures with resolutions of several microns [7-9]. To overcome the low

*Corresponding author. Tel.: +82 51 510 2327, Fax.: +82 51 514 0684
E-mail address: sehlee@pusan.ac.kr
DOI 10.1007/s12206-007-1031-8

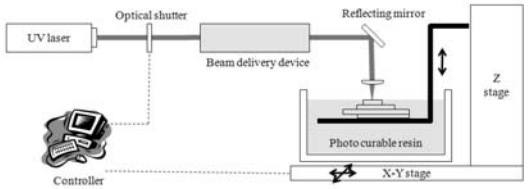

(a) Scanning method

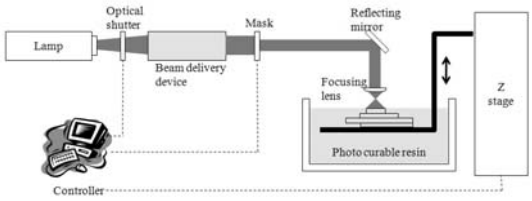

(b) Projection method

Fig. 1. Schematics of the microstereolithography.

contrast and transmittance of LCDs, a digital micromirror device (DMD^{TM}) developed by Texas Instruments has been used as the dynamic pattern generator due to its high contrast and resolution [10-13]. Sun *et al*. [12] produced a suspended beam with a 600 nm diameter, which is the smallest reported feature obtained by using projection MSL processes.

Ikuta *et al*. [2] demonstrated the mass-IH process, which consists of a series of optical fibers and is capable of mass-producing microstructures, but its setup cost is high. Although the achievable resolution of projection MSL is less than that of scanning methods, the use of dynamic masks with high resolution and focusing lenses with high power allows the production of microstructures with high resolution. In this paper, we propose a projection MSL system with uniform illumination and image formation based on optical design software for fabricating microstructure arrays. This system can fabricate 3-D microstructures in the meso-range, which falls between micro- and macro-ranges, with a resolution of a few microns. Microstructure arrays were fabricated to verify the performance of the proposed system.

2. Projection microstereolithography

2.1 System configuration

To implement a MSL apparatus for array fabrication, patterned light must be moved on the resin surface. If the platform attached to the Z stage is moved by using the XY stage, the fabricated part can be damaged by the viscous resin. To avoid this problem, the optical system was mounted on the XY stage. In this way, the Z stage remains immobile so that the fabricated microstructure array cannot be damaged. Such a system configured for microstructure array fabrication is shown in Fig. 2. The system consists of a light source, beam delivery devices, a reflecting mirror, an objective lens, a resin vat, an XY stage, a Z stage, and a control program. The beam delivery devices are composed of a collimating lens set, DMD, and tube lens. To move the optical system, the light source and beam delivery devices are mounted on the XY stage after considering the light path. All of the components on the stage are designed so that their weights do not affect the stage precision.

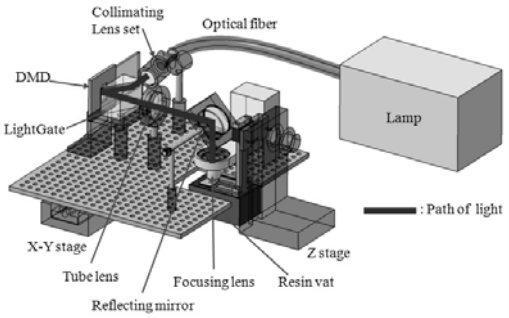

Fig. 2. Schematic of the proposed projection microstereolithography apparatus.

A mercury lamp is used as the light source, which is filtered at a wavelength of 365 ± 10 nm. The emitted light is transferred to one of the beam delivery devices, which consists of a high-pressure optical fiber with a numerical aperture (NA) of 0.37, a working wavelength of 250 to 700 nm, and an output diameter of 8 mm. The electrical shutter is embedded in the lamp and switches the light on and off to transfer the desired energy. The collimating lens set is used to provide uniform illumination because the emitted light from the lamp diverges along the optical axis. A LightGate^{TM} prism made by Unaxis is used to compact the light path, and is coated so that the light is either reflected or allowed to pass through according to the incident angle, as shown in Fig. 3. The reflected light on the prism is directed to the DMD surface. The DMD made by Texas Instruments is used as the dynamic pattern generator. It generates an image of the sliced section by producing a black-and-white region, and reflects the patterned light toward the tube lens. The tube lens is a UV achromat doublet lens with a focal length of 120 mm that delivers the pat-

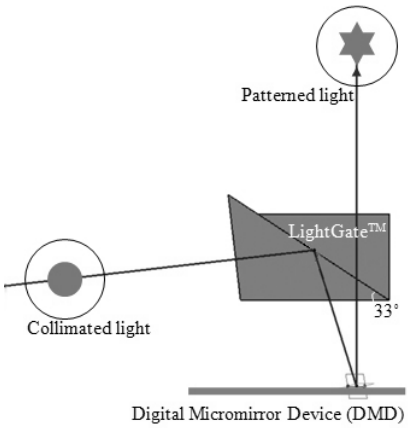

Fig. 3. Light path in the prism (LightGate™).

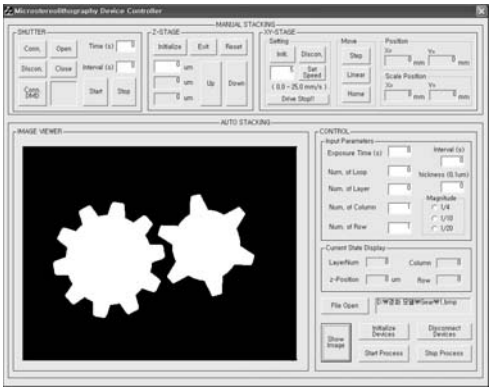

Fig. 4.Control program to fabricate microstructure arrays.

terned light to the reflecting mirror. The reflected light is transferred to the objective lens, which has a NA of 0.3 and a focal length of 20 mm, and a reduced section image is formed on the resin surface. The XY stage, with a resolution of 100 nm and a travel range of 150 mm × 150 mm, enables us to produce microstructure arrays. The Z stage, with a resolution of 100 nm and a travel range of 50 mm, is used to stack the fabricated layers.

Fig. 4 shows the control program developed for microstructure array fabrication. It was implemented in a Windows environment using Visual C++. Every component could be independently controlled by manual operations and microstructure arrays could be fabricated by inputting the number of rows and columns.

2.2 Fabrication process

The fabrication process is similar to that of conventional stereolithography systems. The object to be fabricated is modeled by CAD software, and the resulting file is converted to a STL format, which consists of triangle facets. Two-dimensional cross-sectional data are generated by slicing the STL file according to the layer thickness to generate bitmap images for input to the DMD. The bitmap of each layer is symmetrized about the center point of the image while considering the formed image on the resin surface. The array fabrication starts by initializing the devices after inputting the number of rows and columns. The bitmap image corresponding to the cross section is transferred to the DMD, and the patterned light is projected on the resin surface. The patterned light is then moved to another position by the XY stage while the shutter is closed, and projected again when the shutter is open. One layer is cured as these processes continue according to the desired number of rows and columns. After each section of one layer is fabricated, the XY stage returns to its home position. The Z stage moves up and down according to the layer thickness to refresh the resin surface. Ten seconds, estimated empirically, are required to flatten the unstable resin surface. To fabricate a new layer, the next bitmap image is transferred to the DMD, and the above process is repeated. Once all layers have been fabricated, the part is pulled out of the plate and rinsed. The overall process for micro-

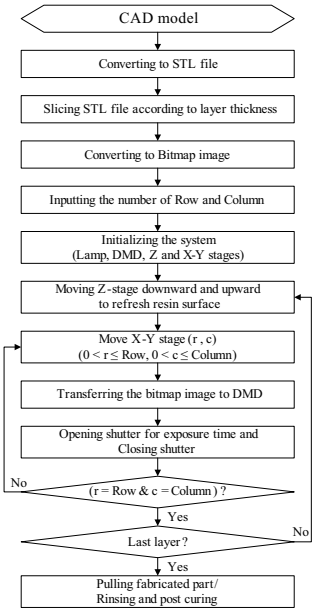

Fig. 5. Overall process for fabricating microstructure arrays.

structure array fabrication is shown in Fig. 5.

3. Optical design

To install each component at specific positions, the uniform illumination and image formation are taken into consideration. The movement of the XY stage is also considered because the optical components mounted on the XY stage affect the fabrication precision. The uniform illumination is a part of the irradiation onto the DMD while the image formation is a part of the system used to deliver and focus the patterned light reflected from the DMD on the resin surface.

3.1 Uniform illumination

Most of the optical components were mounted on the XY stage. These components must be compact since they can affect the fabrication precision. Therefore, the light path must be shortened. The illumination distance can be shortened by using a prism and a collimating lens set composed of two convex lenses with short focal lengths. The collimating lens set, DMD and prism have to be installed at specific positions according to the light path. To simplify the design of the light path, the center of the DMD surface is located in the origin of the 3-D coordinate systems, the reflected light from the DMD is horizontal and the principal ray of the light is only considered. Fig. 6 shows the positions of each component according to light path.

A procedure to determine the specific positions of the components is as follows. First, the reflected ray from the DMD (*Ray0*) is considered. The unit vector of the *Ray0* ($\mathbf{U_0}$) is easily obtained because it has the inverse direction compared with the unit normal vector of the YZ plane; $\mathbf{U}_0 = (-1, 0, 0)$

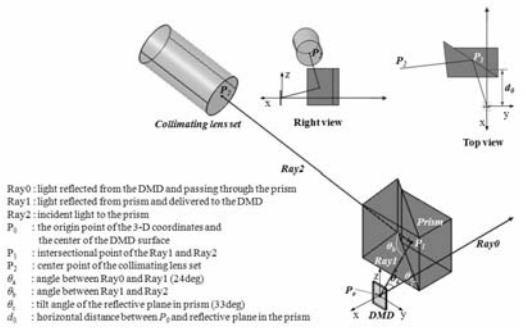

Fig. 6. Positions of each component according to the light path.

Second, the ray delivered to the DMD after being reflected from the prim (*Ray1*) is considered. The unit vector of the *Ray1* ($\mathbf{U}_1$) is calculated by the dot product between the unit normal vector of the tilting plane of the DMD ($\mathbf{N}_t$) and the unit vector $\mathbf{U_0}$ because the *Ray0* and the *Ray1* make the same angle with respect to the unit normal vector $\mathbf{N}_t$. At this time, each micromirror in the DMD is tilted at ±12 degrees along by the diagonal axis, so the angle between *Ray0* and *Ray1* (θ_a) is 24 degrees [14]. So, these vectors are described by

$$\mathbf{N}_t = \left(\cos\frac{\theta_a}{2},\ \sqrt{\frac{1-\cos^2\frac{\theta_a}{2}}{2}},\ -\sqrt{\frac{1-\cos^2\frac{\theta_a}{2}}{2}} \right) \quad (1)$$

$$\mathbf{U}_1 = \left(\cos\theta_a,\ \sqrt{\frac{1-\cos^2\theta_a}{2}},\ -\sqrt{\frac{1-\cos^2\theta_a}{2}} \right) \quad (2)$$

Third, the point (P_1) can be derived by intersecting the reflective plane inside of the prism and *Ray1*. The prism was set parallel with respect to the DMD surface, so the tilt angle of the reflective plane (θ_c) is 33 degrees. The point (P_1) could be changed according to the distance between the center of the DMD surface and the reflective plane along by the x-direction (d_0). In our study, the d_0 was set to 31.5 mm considering the divergence of the reflected light from the DMD. The unit normal vector of the reflective plane ($\mathbf{N}_r$) is described by

$$\mathbf{N}_r = \left(\frac{1}{\sqrt{1+\tan^2\theta_c}},\ \frac{-\tan\theta_c}{\sqrt{1+\tan^2\theta_c}},\ 0 \right) \quad (3)$$

The point P_1 is determined to be (-39.588, -12.463, 12.463). Fourth, the ray irradiated from the collimating lens set (*Ray2*) is considered. The unit vector of the *Ray2* ($\mathbf{U}_2$) can be also calculated by three conditions: (1) the magnitude of the unit vector (U_{2x}, U_{2y}, U_{2z}) is 1; (2) the *Ray1* and the *Ray2* make the same angle with respect to the unit normal vector $\mathbf{N}_r$; and (3) the vectors, $\mathbf{U}_1$, $\mathbf{U}_2$ and $\mathbf{N}_r$ lie on the same plane. These conditions are described by

$$\begin{aligned} &U_{2x}^2 + U_{2y}^2 + U_{2z}^2 = 1 \\ &\mathbf{U}_1 \cdot \mathbf{N}_r = \mathbf{N}_r \cdot \mathbf{U}_2 \\ &\cos\frac{\pi}{2} = \mathbf{U}_2 \cdot (\mathbf{N}_r \times \mathbf{U}_1) \end{aligned} \quad (4)$$

The resultant unit vector $\mathbf{U}_2$ is determined to be

(-0.0186, 0.952, -0.2877). Finally, the line equation of the *Ray2* derived from the unit vector $\mathbf{U}_2$ and the point P_1 can be described by

$$\frac{x+39.588}{-0.1086}=\frac{y+12.463}{0.952}=\frac{z-12.463}{-0.2877} \quad (5)$$

Therefore, the position of the collimating lens set (P_2) could be estimated by Eq. (5) and the focal length of that [15]. In our study, the point P_2 is determined to be (-28.461, -110, 41.939), respectively.

Uniformly collimated light from the collimating lens set is delivered to the prism. The reflected light from the prism is directed to the DMD surface, then only light patterned by the DMD is passed through the prism. To avoid nonuniform illumination, 800 × 600 pixels of the DMD were used. To confirm that the prism and DMD were working correctly, a rectangular light pattern with 800 × 600 pixels was measured before the tube lens by using a beam profiler (FX66, Ophir Optronics). The results, shown in Fig. 7, give an average light intensity of 0.0148 W/cm^2, which was almost uniform for the entire active area of the DMD.

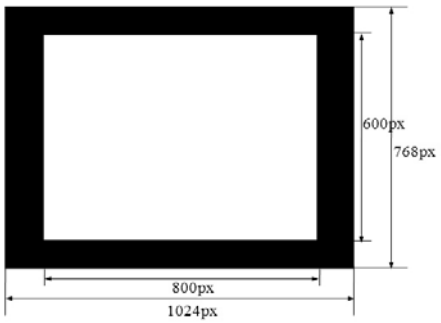

(a) Rectangular image on the DMD

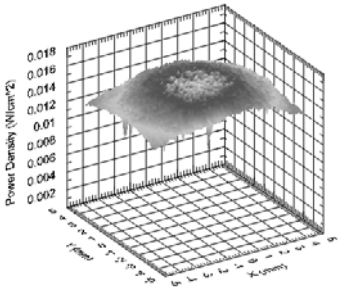

(b) 3-D beam profile measured by FX66

Fig. 7. Verification of the uniform illumination according to the light path.

3.2 Image formation

The light patterned by the DMD tends to diverge, so a tube lens is used to collimate the light. The horizontal light is reflected by the UV mirror, and delivered vertically to the objective lens. Photopolymerization occurs on the resin surface with a reduced size according to the magnification. As shown in Fig. 8, the distance between the DMD and the tube lens (z_{dt}) must be the same as the focal length of the tube lens for collimation. The distance between the tube lens and the objective lens (z_{to}) can vary so that the components can fit into the overall configuration. The distance between the objective lens and resin surface must be the same as the working distance of the objective lens so that its focal length (f_o) will fit into the space.

To optimize the distances, an optical simulation was performed by using ZEMAX, which is a commercial software package for optical design. We assumed that the reflected light on the DMD was a set of point sources, the objective lens reduced all aberrations, and all rays could be followed by a paraxial formula. The reflecting mirror was not considered because it only changes the path of the light. Optimized values of the distances z_{dt} and z_{to} were estimated to be 115.2 mm and 186.5 mm, respectively, yielding a magnification for image formation of 0.174 from the lens formula f_o/z_{dt} [15].

4. Microstructure array fabrication

4.1 Fabrication resolution

In this system, the bitmap image is used as a fabrication data. Therefore, the conversion of sliced cross-section data into bitmap images is needed. At this time, one pixel of bitmap image is corresponding to one micrometer of sliced data. The fabrication resolution of the proposed projection MSL system is determined by the resolution of the dynamic mask, power of the objective lens, and curing characteristics of the photocurable resin. The DMD used to generate the dynamic pattern consists of 1024×768 micromirrors

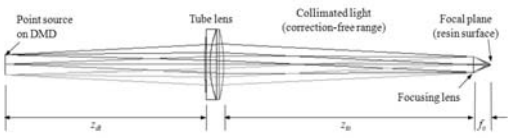

Fig. 8. Optimized lens position for image formation [14].

and each micromirror has dimensions of 13.68 μm per side. When using a 10× objective lens, the theoretical value of projected image size and resolution is 1.40 mm×1.05 mm and 1.368 μm, respectively. To estimate the real fabricable resolution of the system, a 2-D line pattern was fabricated more than ten times. The line width varied from 6 pixels to 1 pixel in pairs. Fig. 9(a) shows the bitmap image and fabricated line pattern after rinsing with isopropyl alcohol (IPA). One pixel line, measured with a microscope (DFC 280, Leica) was averagely 2 μm, which is 1.46 times of the theoretical value and twice of the designed value. In case of array fabrication for mass production, after fabricating one layer, the XY stage must move to the same irradiation position as the previous layers in order to maintain the designed shape. The position error range was controlled within ±100 nm. A bitmap image composed of five circles with diameters of 100 pixels was used to verify the accuracy of the XY stage, as shown in Fig. 9(b). The fabricated structures consisted of 100 layers with 10 μm layer thicknesses, with three rows and columns. The measured diameter and height of the structures were 200 μm and 1070 μm, respectively. The results indicate that the fabricated parts had the same dimensions and the shapes were well maintained.

At this experiment, a blended prepolymer of isobornyl acrylate $C_{13}H_{20}O_2$ (IBXA), 1,6-hexanediol diacrylate (HDDA), and bisphenol-ethoxylated (4) diacrylate (BED) was used as the photocurable resin.

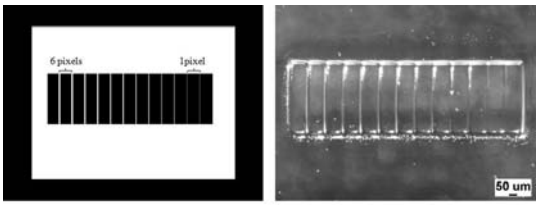

(a) 2D line patterns varied from 6 pixels to 1pixel and fabricated patterns

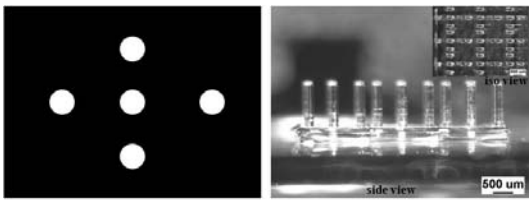

(b) Circles with diameters of 100 pixels and fabricated cylinder arrays of 3×3

Fig. 9. Test model to achieve the fabrication resolution for the proposed system.

The ratio of IBXA:HDDA:BED was 80:10:10%. Then, 2 wt% of tetraethoxyorthosilicate (TEOS) for improving the mechanical properties, 5 wt% of 2,2-dimethoxy-2-phenylacetophenone (DMPA) for initiating the photopolymerization, and 0.1wt% of tinuvin for absorbing the photonic energy to reduce the curing depth were added [15].

4.2 Fabrication examples

Microstructures arrays were fabricated by the developed projection MSL system. Fig. 10 shows examples of the fabricated microstructure arrays. The micro-glass array shown in Fig. 10(a) is a 5×5 structure with a fabrication range of 10 mm×10 mm at the bottom. The layer thickness is 5 μm and the total number of layers is 300. The designed outer diameter is 500 μm on the top and a wall thickness is 40 μm. After fabricating, the measured dimensions were 1,000 μm and 80 μm, respectively. Fig. 10(b) shows a 3×3 micro-bishop array. The fabrication range is 5.1 mm×3.7 mm, the layer thickness is 20 μm, and the total number of layers is 134. The designed diameter on the top is 100 μm and the diameter at the bottom is 600 μm. The measured dimensions were 200 μm and 1,200 μm, respectively. The fabrication parameters and characteristics of the microstructure arrays are listed in Table 1.

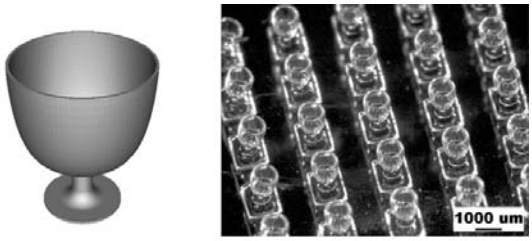

(a) Micro-glass CAD model and fabricated array

(b) Micro-bishop CAD model and fabricated array

Fig. 10. Fabrication of microstructure arrays.

Table 1. Fabrication parameters and characteristics of microstructure arrays.

Parameters \ Model	Micro-glass	Micro-bishop
Num. of layer	300	134
Slicing thickness(μm)	5	20
Fabrication range(mm)	10×10	5.1×3.7
Num. of rows and columns	5×5	3×3
Intensity(mW/cm^2)	56.4	56.4
Fabrication time(hrs)	8.3	2.7

All fabricated microstructures were the same as each other, and were maintained twice the designed dimension. The overhanging shapes inside the microstructures were also well maintained. These examples demonstrate that the developed MSL system effectively fabricated the microstructure arrays and showed the mass producibility of a microstructure as increasing the number of rows and columns. The results suggest that the system could be used to fabricate microstructures with a resolution of a few micrometers within several tens of millimeters.

5. Conclusions

A projection MSL system for mass production of microstructures was proposed and verified experimentally. To shorten the distance of the light path and create a compact configuration, a collimating lens set and prism were added to the system. The beam profile was measured to verify the uniform illumination and evaluate the prism performance. The light path was analyzed, and all of the components were installed at specific positions so that the incident light on the DMD would be uniform. The tube lens, reflecting mirror, and objective lens were positioned by using an optical design software package. The fabricated 2-D line pattern was measured to ensure that a fabricable resolution was achieved. Arrayed 3-D microstructures were successfully fabricated according to the desired number of rows and columns. The proposed system enables one-stop fabrication of various microstructures when using several section images for one layer.

Acknowledgments

This work was supported by grant No. R01-2004-000-10507-0 from the Basic Program of the Korea Science & Engineering Foundation.

References

[1] V. K. Varadan, X. Jiang and V. V. Varadan, Microstereolithography and other Fabrication Techniques for 3D MEMS, John Wiley & Sons, West Sussex, England, (2001).

[2] K. Ikuta and K. Kirowatari, Real three dimensional micro fabrication using stereo lithography and metal molding, Proc. of the IEEE MEMS'93, Fort Lauderdale, New York, USA. (1993) 42-47.

[3] K. Ikuta, T. Ogota, M. Tsubio and S. Kojima, Development of mass productive micro stereolithography, Proc. of the IEEE MEMS'96, San Diego, USA. (1996) 301-306.

[4] X. Zhang, X. N. Jiang and C. Sun, Microstereolithography of polymeric and ceramic microstructures, *Sensor. Actuat. A-Phys.* 77 (2) (1999) 149-156.

[5] I. H. Lee and D. W. Cho, An investigation on photopolymer solidification considering laser irradiation energy in micro-stereolithography, *Microsyst. Technol.* 10 (8) (2004) 592-598.

[6] A. Bertsch, S. Zissi, J. Y. Jezequel, S. Corbel and J. C. Andre, Microstereophotolithography using a liquid crystal display as dynamic mask-generator, *Microsyst. Technol.* 3 (2) (1997) 42-47.

[7] M. Farsari, F. C. Tournier, S. Huang, C. R. Chatwin, D. M. Budgett, P. M. Birch, R. C. D. Young and J. D. Richardson, A novel high-accuracy microstereolithography method employing an adaptive electro-optic mask, *J. Mater. Process. Tech.* 107 (1) (2000) 167-172.

[8] C. Provin and S. Monneret, Complex Ceramic-Polymer Composite Microparts Made by Microstereolithography, *IEEE T. Electron. Pack.* 25 (1) (2002) 59-63.

[9] G. Oda, T. Miyoshi, Y. Takaya, T. H. Ha and K. Kimura, Microfabrication of overhanging shape using LCD microstereolithography, Proc. of SPIE 5662, Bellingham, WA, USA. (2004) 649-654.

[10] A. Bertsch, P. Bernhard, C. Vogt and P. Renaud, Rapid prototyping of small size objects, *Rapid Prototyping J.* 6 (4) (2000) 259-266.

[11] A. Bertsch, S. Jiguet and P. Renaud, Microfabrication of ceramic components by microstereolithography, *J. Micromech. Microeng.* 14 (2) (2004) 197-203.

[12] C. Sun, N. Fang, D. M. Wu and X. Zhang, Projection micro-stereolithography using digital micro-mirror dynamic mask, *Sensor. Actuat. A-Phys.* 121 (1) (2005) 113-120.

[13] J. W. Choi, Y. M. Ha, M. H. Won, K. H. Choi and S. H. Lee, Fabrication of 3-dimensional microstructures using dynamic image projection, Proc. of the ASPEN'2005, Shenzhen, China. (2005) 472-476.

[14] J. W. Choi, Y. M. Ha, S. H. Lee and K. H. Choi, Design of microstereolithography system based on dynamic image projection for fabrication of three-dimensional microstructures, *J. Mech. Sci. Technol.* 20 (12) (2006) 2094-2104.

[15] J. W. Choi, Development of projection-based microstereolithography apparatus adapted to large Surface and microstructure fabrication for human body application, Ph. D. Dissertation, Pusan National University, (2007).